Melamine Structures on the Au(111) Surface

Fabien Silly,*,†,‡ Adam Q. Shaw,† Martin R. Castell,† G. A. D. Briggs,† Manuela Mura,§ Natalia Martsinovich,§ and Lev Kantorovich§,⊥

Department of Materials, University of Oxford, Parks Road, Oxford OX1 3PH, U.K., Zernike Institute for Advanced Materials, Rijksuniversiteit Groningen, Nijenborgh 4, NL-9747 AG, Groningen, The Netherlands, and Department of Physics, King's College London, The Strand, London, WC2R 2LS, U.K.

Received: April 18, 2008; Revised Manuscript Received: May 23, 2008

We report on a joint experimental and theoretical study of the ordered structures of melamine molecules formed on the Au(111)-(22 × $\sqrt{3}$) surface. Scanning tunneling microscopy (STM) images taken under UHV conditions reveal two distinct monolayers one of which has never been reported before on gold. We also find that one of the structures may serve as a transition region ("domain wall") between islands formed by the other arrangement. Using state-of-the-art density functional calculations in conjunction with a systematic gas-phase analysis based on considering all planar structures melamine molecules can form with each other, we propose atomistic models for both structures and the transition region.

An ability to control molecular ordering on surfaces is a key requirement in producing molecular devices. Self-assembly techniques may provide a solution to this and are, therefore, under intense investigation. The precise positioning of molecules on a large scale can be achieved using substrate properties[1–8] and by exploiting intermolecular interactions to form extended networks.[9–13] From this point of view, the small highly symmetrical triangle-shaped melamine (1,3,5-triazine-2,4,6-triamine) is of primary interest. This nonchiral molecule can form a chiral network[14–16] on metal surfaces and has an ability to successfully mix with other molecular blocks, such as PTCDI,[13–15,17,18] NTCDI,[19] PTCDA,[20,21] and cyanuric acid[16,22] whereby creating complex supramolecular architectures with either nonchiral or chiral symmetry. The understanding of the molecular binding is therefore essential in order to predict and control assemblies of this molecule. Melamine molecules can form hydrogen bonds with each other, so that, depending on the particular arrangement of molecules, various assemblies are possible with varying stabilities. To our knowledge, only one pure melamine self-assembled structure has been reported so far[14–16] on Au(111) surface.

In this paper, we report on the ordering of melamine molecules, shown in Figure 1, on the Au(111) surface. We have found, using scanning tunneling microscopy (STM) imaging in ultrahigh vacuum (UHV), that melamine can form at least two different periodic structures, from which only one is chiral. Using state-of-the-art density functional calculations and a systematic topological analysis, we propose atomistic models for the observed monolayers.

We used Au(111) films grown on mica. The samples were introduced into the UHV chamber of an STM (JEOL JSTM4500S) operating at a pressure of 10^{-8} Pa. The Au(111) surfaces were sputtered with argon ions and annealed in UHV at temperatures between 600 and 800 °C, typically for 30 min. Melamine molecules were sublimated at 100 °C. Etched tungsten tips were used to obtain constant current images at room temperature with a bias voltage applied to the sample. STM images have been processed and analyzed with FabViewer.[23]

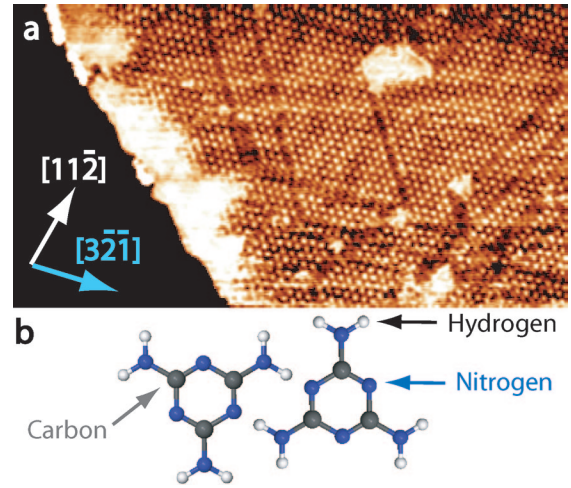

Figure 1. (a) Melamine domains on a Au(111) surface (55 × 30 nm^2; $V_s = -1.5$ V, $I_t = 0.1$ nA). (b) Melamine molecule model.

Figure 1a shows a large scale STM image of the Au(111) surface after deposition of melamine. The surface is covered by a hexagonal network, which is crossed by stripes. These stripes, which run along the [3$\bar{2}\bar{1}$] direction on the reconstructed Au(111) surface, form geometric shapes resembling equilateral triangles and parallelograms. The reconstructed "herringbone"[24] Au(111) surface is visible in Figure 1a, indicating a rather weak interaction of the melamine with the gold. White areas in the STM image correspond to the bare gold surface.

Figure 2a is a high resolution STM image of the hexagonal ordering observed in Figure 1a. Melamine molecules form domains of linked hexagons each composed by six melamine molecules.[14,15,21] The model representing the observed melamine arrangement is shown in Figure 2b. In this model the melamine arrangement is stabilized by double hydrogen bonds between melamine molecules. Conflicting results were published about melamine orientation on this surface. In refs 16 and 25, centers of hexagons of melamine network were found to be aligned

* Corresponding author. E-mail: f.n.silly@rug.nl.
† Department of Materials, University of Oxford.
‡ Zernike Institute for Advanced Materials, Rijksuniversiteit Groningen.
§ Department of Physics, King's College London.
⊥ E-mail: lev.kantorovitch@kcl.ac.uk.

10.1021/jp8033769 CCC: $40.75 © 2008 American Chemical Society
Published on Web 07/03/2008

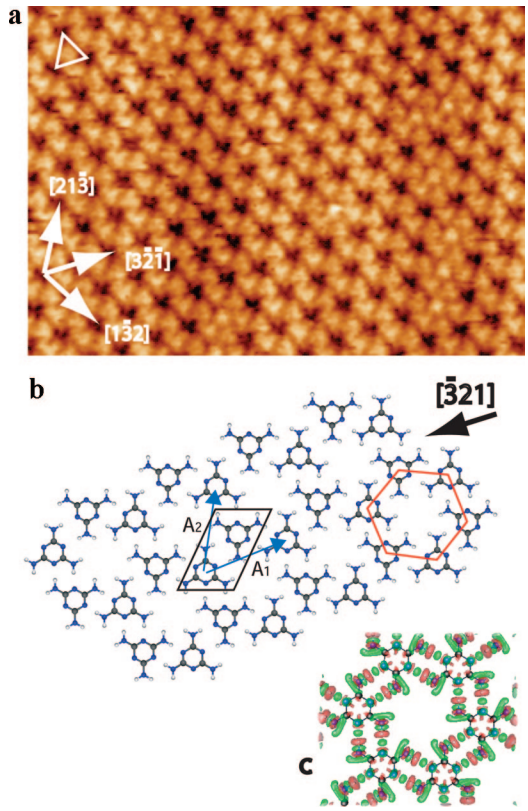

Figure 2. (a) STM image of a melamine domain on a Au(111)-(22 × $\sqrt{3}$) surface (13 × 9 nm^2; V_s = −1.1 V, I_t = 0.5 nA), (b) the corresponding molecular model consisting of hexagons and (c) the electron density difference plot, corresponding to ±0.01 electrons. In the density plot green surfaces correspond to the regions of positive electron density difference (excess), whereas red areas correspond to the regions of negative electrons density difference (depletion).

along the [11$\bar{2}$] and [$\bar{4}$13] directions, respectively, while in ref 22 melamine forms a very large supercell of the commensurate structure with the direction between the nearest hexagons of melamine making about 15° to the [10$\bar{1}$] direction. The visible Au(111) reconstruction underneath the melamine layer in Figure 1 shows that in our experiments the melamine hexagon centers are aligned in the [3$\bar{2}\bar{1}$] direction (Figure 2a). The average melamine hexagon center-center separation is measured to be 9.6 Å in the [3$\bar{2}\bar{1}$], 9.8 Å in the [1$\bar{3}$2] and 10.0 Å in the [21$\bar{3}$] directions. The variety of possible directions found in these studies indicates that the alignment of the melamine monolayer with respect to the gold surface may be influenced by the surface preparation.

Figure 3a shows a domain of a new close-packed melamine ordering (circled) which coexists with the hexagonal one shown on the right of the same image. In the close-packed structure melamine molecules form domains of multiple rows aligned in the [12$\bar{3}$] direction. The unit cell of this melamine network, indicated in Figure 3a, has a shape of a parallelogram with dimensions of 8.0 Å in the [12$\bar{3}$] direction and 9.8 Å along the direction making a 5° angle with the [$\bar{3}$21] direction. The close-packed structure was mostly observed at high coverages (close to one monolayer), and may represent up to 5% of the whole layer. It is mostly seen at the boundaries between hexagonal domains. Distorted close-packed melamine structure was observed on Ag−Si(111) but was suggested to result from the interaction with the surface.[19]

Figure 4a shows a high resolution image of the stripes running in the [3$\bar{2}\bar{1}$] direction of the reconstructed Au(111) surface, observed in Figure 1a. It is seen that these stripes actually appear

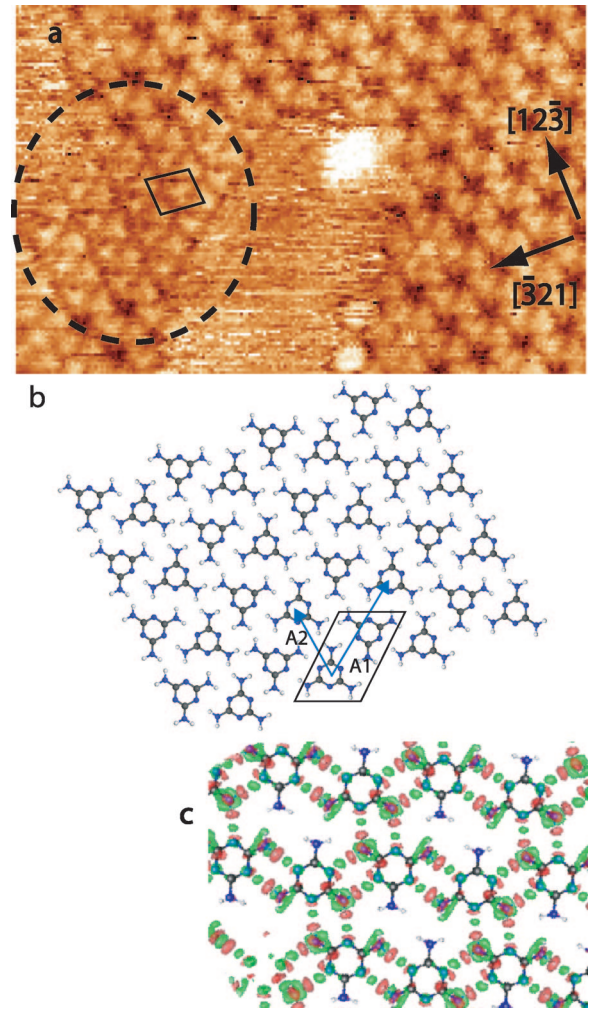

Figure 3. (a) STM image of a melamine domain on a Au(111) surface (12 × 8 nm^2, V_s = −1.1 V, I_t = 0.5 nA.), (b) molecular model of the melamine domain, and (c) the electron density difference plot corresponding to the circled region in part (a).

as a boundary (highlighted by an arrow in Figure 4a) between two melamine hexagonal domains. A close inspection of the triangular features in the boundary region suggests that the melamine molecules are close-packed there; in fact, one may assume that the boundary represents a two-molecule filament extracted from the close-packed structure circled in Figure 3. The periodicity along the arrow is 9.8 Å for both structures (the hexagonal and the stripe).

To model the experimentally observed melamine ordering we performed calculations using an *ab initio* SIESTA method,[27,28] based on localized numerical orbital basis set, periodic boundary conditions and the first-principles scalar-relativistic norm-conserving[29,30] Troullier-Martins[31] pseudopotentials factorized in the Kleinman−Bylander[32] form. We used the Perdew, Becke, and Ernzerhof (PBE)[34] generalized gradient approximation for the exchange and correlation which was found previously to be adequate in representing hydrogen bonding between DNA bases molecules.[35] In each calculation, atomic relaxation was performed until the forces on atoms were less than 0.01 eV/ Å.

In order to build all possible structures we used a systematic approach[35] which consists of the following steps: (i) all sites on a periphery of the molecules, which can participate in a hydrogen bonding with another molecule, are identified; (ii) all possible dimers are constructed (only one is possible in the case of melamine[14]); (iii) by connecting molecules using dimers rules,

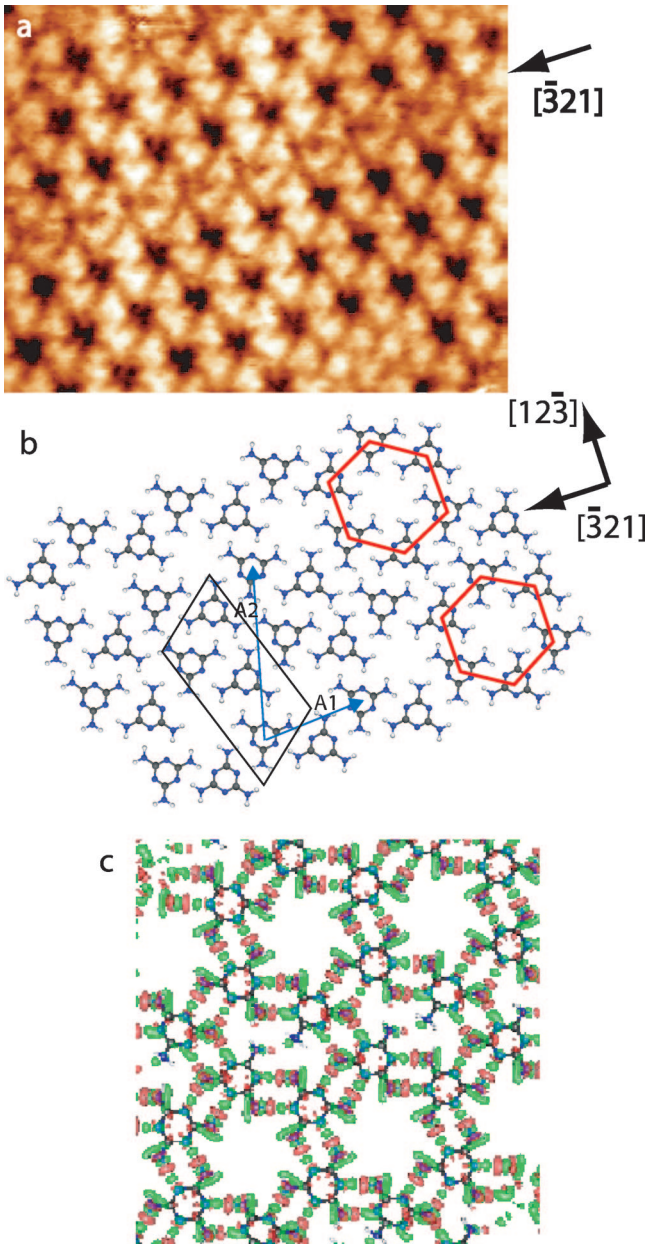

Figure 4. (a) STM-image of a melamine domain on a Au(111) surface ($V_s = -1.1$ V, $I_t = 0.5$ nA, 8×6 nm ^{2}). (b) Molecular model and (c) the electron density difference plot of the region along the arrow in part a. (The theoretical lattice vectors are as follows: $A_1 = 10.65$ Å, $A_2 = 17.69$ Å; the angle between them is 51.3°).

all possible unit cells are constructed; (iv) all possible one-dimensional chains are constructed based on every unit cell; (v) by attaching chains parallel to each other, all possible two-dimensional periodic structures are formed with the preselected number of molecules in the unit cell; (vi) stabilities of all assemblies are estimated by summing up all dimer energies (per cell); finally, (vii) the most stable structures are then fully relaxed using the *ab initio* method. Then, if necessary, the calculated structures are corrected by estimating their interaction with the substrate.

The energetics of each gas-phase monolayer, calculated using SIESTA, is characterized by its stabilization energy which is composed of two components: the interaction and deformation energies. If the former characterizes the strength of intermolecular interaction (it is negative), the latter shows the energy penalty due to inevitable deformation of molecules in the final

TABLE 1: Energies (per cell) of the Monolayers Built with Two Molecules Per Unit Cell[a]

	hexagonal	close-packed
E_{stab} (eV)	−1.29	−0.99
E_{int} (eV)	−1.67	−1.28
E_{def} (eV)	0.38	0.29
$E_{H\text{-}bond}$ (eV)	−0.22	−0.17

[a] The stabilization energies include the BSSE correction. The bottom row represents the average energy per single hydrogen bond in the structure.

structure (and is positive). The calculated energies include the basis set superposition error (BSSE) correction[33] due to the localized basis set used. To analyze bonding in the relaxed structures, the electron density difference (between the total density and that of all individual molecules in the geometry of the combined system) was found to be especially useful since the hydrogen bonding is known[35] to be well characterized by the "kebab" structure associated with alternating regions of excess and depletion of the electron density along the donor-hydrogen-acceptor line of atoms.

In order to interpret the observed images, we first note that each melamine molecule has six equivalent sites which are able to form a double hydrogen bond with a similar site of another melamine molecule, Figure 1b. The dimer binding energy we find is −0.48 eV (−0.24 eV per one hydrogen bond). Assuming that there are only two molecules in the two-dimensional unit cell, we have found, using our systematic method, that *only two* monolayers are actually possible: (i) the hexagonal structure shown in Figure 2(b) which is the same as the one suggested previously,[14–16,21,25] and (ii) a new close-packed arrangement, the relaxed structure of which is shown in Figure 3b. The small number of possibilities is explained by the high symmetry of the melamine molecule. If the hexagonal structure is *nonchiral*, the close-packed one is *chiral*, as the latter monolayer when flipped cannot be made identical to the original one by means of any rotations and/or translations.

The energetics of both structures is shown in Table 1. One can see that the hexagonal structure is more stable. Since the deformation energies in the closed-packed structure is by 0.1 eV smaller than in the hexagonal one, the main gain for the latter arrangement originates from the much more preferable intermolecular interaction. Electron density difference plots shown in Figures 2c and 3c, demonstrate that in the case of the close-packed structure some of the hydrogen bonds are much weaker: one (out of three) amino-group of each molecule participates at the same time in two hydrogen bonds making it difficult for the corresponding nitrogen donor to provide enough electron density to the bonds. In addition, there is also a steric effect: some of the hydrogen atoms in the close-packed structure are too close in distance, consequently, in order to minimize the deformation energy, the hydrogen atoms of neighboring molecules move away from the molecular plane in the opposite directions. All these factors make the close packed structure less stable than the hexagonal one, however, it is much denser and allows a more efficient packing of the molecules. This is in agreement with our observations, reported above, that the close-packed structure is seen mostly at large coverages as a boundary region between two hexagonal arrangements.

The calculated lattice parameters of the two structures, which are shown in Table 2, compare well with those measured experimentally. We have also checked that the relaxed structures match well with the observed ones if overlaid on their images, suggesting that they represent the correct models for the observed monolayers.

TABLE 2: Comparison between the Theoretical (Assuming Two-Molecule Unit Cells) and the Experimental Lattice Parameters for the Two Monolayers

	lattice vector A_1 (Å)	Lattice vector A_2 (Å)	angle (deg)
hexagonal (theory)	10.66	10.66	60
hexagonal (experiment)	10 ± 1	10 ± 1	60 ± 2
close-packed (theory)	12.00	7.68	65.3
close-packed (experiment)	13 ± 1	8 ± 1	63 ± 4

By assuming a larger number of the molecules in the unit cell, more monolayers can be constructed. Due to a specific symmetry of the melamine molecule, it can be checked that it can only be possible to construct a periodic two-dimensional structure with an *even* number of molecules in the cell. Now, assuming four molecules in the cell, we find 11 possible unit cells which can be used to construct eight different monolayers. Note, however, that only three monolayers out of these have high stabilities due to each molecule being "connected" by hydrogen bonds with three neighboring molecules; in other monolayers some of the molecules are connected only to two neighbors. One example hexagonal structure corresponding to four molecules in the cell is shown in Figure 4b. This particular structure is quite peculiar: it consists of elements of both monolayers (which were based on two-molecules cells) considered above. Indeed, one can see hexagons and close-packed rows of molecules with some of their amino groups participating in two double hydrogen bonds at the same time. In addition, in this structure, as well as in the close-packed monolayer of Figure 3b, some of the hydrogens are positioned very close to each other forcing them to move out of the molecular plane to relieve strain in the system. One can also appreciate that this structure is quite stable with the stabilization energy of -1.36 eV per two molecules (this is even slightly more stable than the hexagonal structure of Figure 2b). This four-molecule structure can serve as an atomistic model for the closed-packed boundary region shown in Figure 3.

The simulation of monolayers presented above has been done in the gas phase, assuming that the interaction between molecules is of primary importance. We have checked this assumption by considering, first, a single molecule and then its dimer at various positions on the surface and either relaxing them or performing constant temperature (up to 300 K) molecular dynamics simulations. We find that the potential energy surface calculated with DFT is very flat, i.e. its corrugation across the surface does not exceed 0.05 eV, the more stable positions being those where a nitrogen atom of one of the NH_2 groups is above a gold atom. In all cases a single molecule lies flat at a distance of about 3.5 Å from the surface and the binding energy of around -0.2 eV practically does not depend on the molecule's lateral position. When considering a dimer on the surface, similar results with planar dimers have been obtained. However, we have also found dimer geometries in which one of the NH_2 groups participating in the intermolecular bonding is slightly bent toward the surface (its nitrogen atom is positioned directly above a Au surface atom at a distance of 2.6 Å) with a very small gain in the binding energy of -0.07 eV per molecule.

It is well-known[36,37] that the van der Waals (vdW) interaction is not accounted for in the PBE functional we used. Therefore, second, in order to check whether the vdW interaction between the surface and a melamine molecule is important, we calculated the interaction energy between a single molecule and the gold surface using a potential which approximately takes account of the vdW interaction.[38] Although we found that the adsorption energy of a single melamine molecule on the surface comes out much larger (around -1.1 eV) than in our DFT calculations, its corrugation across the surface was obtained to be still not larger than 0.04 eV. We conclude that most likely the vdW interaction between the surface and the molecule does not contribute significantly to the corrugation of the surface potential; i.e., it is still rather flat.

These results indicate that interaction of a melamine molecule with the Au(111) surface does not change significantly with the actual position of the molecule on the surface; moreover, the surface practically does not influence the ability of the melamine molecules to form dimers and thus more complicated structures. In order to understand the preferential orientations of the observed melamine assemblies, we note that the interaction energy of larger melamine clusters (containing more than two molecules) with the surface may have much larger corrugation. Specifically, it is possible that preferential network geometries involve special alignments of nitrogen atoms of NH_2 groups of the melamine molecules with the surface Au atoms. Therefore, we propose that preferential orientation of the islands happens when they grow at room temperature during the deposition: initially, small clusters are formed; then, as more molecules are being attached to the clusters, the clusters start to move around to minimize their free energy and then continue growing without changing their orientation anymore.

In this paper we reported on the deposition of melamine on the Au(111) surface. We observed that melamine can form two different networks, one hexagonal and another close-packed and that a transition region may be formed between different hexagonal islands which has the close-packed structure. The appearance of this kind of boundary is most probably related to the kinetics of the monolayer formation. Initially, when more stable hexagonal islands are formed, their nucleation may happen at various surface sites due to weak dependence of the molecules binding energy on their lateral position. When the coverage is increased, the boundaries of growing islands come close to each other and there may not be enough space to smoothly close the gap between them. Then, the close-packed boundary, which occupies less space and is still rather stable, is formed instead. Therefore, the close-packed structure may indeed appear as a transition region (or a "domain wall") between two more stable hexagonal islands.

Acknowledgment. The authors thank the EPSRC (EP/D048761/1 and GR/S15808/01) for funding, Chris Spencer (JEOL U.K.) for valuable technical support and Stefano Piana (Curtin University of Technology Australia) for his help with classical potential simulations.

Supporting Information Available: Images of the calculated six melamine monolayers having high stabilities due to each molecule being "connected" by hydrogen bonds with three neighboring molecules. This information is available free of charge via the Internet at http://pubs.acs.org.

References and Notes

(1) Dil, H.; Lobo-Checa, J.; Laskowski, R.; Blaha, P.; Berner, S.; Osterwalder, J.; Greber, T. *Science* **2008**, *309*, 1824.

(2) Deak, D. S.; Silly, F.; Porfyrakis, K.; Castell, M. R. *J. Am. Chem. Soc.* **2006**, *128*, 13976.

(3) Sakurai, T.; Wang, X. D.; Xue, Q. K.; Hasegawa, Y.; Hashizume, T.; Shinohara, H. *Prog. Surf. Sci.* **196**, *51*, 263.

(4) Katano, S.; Kim, H.; Matsubara, Y.; Kitagawa, T.; Kawai, M. *J. Am. Chem. Soc.* **2007**, *129*, 2511.

(5) (a) Silly, F.; Pivetta, M.; Ternes, M.; Patthey, F.; Pelz, J. P.; Schneider, W.-D. *Phys. Rev. Lett.* **2004**, *92*, 016101. (b) Silly, F.; Pivetta, M.; Ternes, M.; Patthey, F.; Pelz, J. P.; Schneider, W.-D. *New J. Phys.* **2004**, *6*, 16.

(6) Wang, W. C.; Zhong, D. Y.; Zhu, J.; Kalischewski, F.; Dou, R. F.; Wedeking, K.; Wang, Y.; Heuer, A.; Fuchs, H.; Erker, G.; Chi, L. F. *Phys. Rev. Lett.* **2007**, *98*, 225504.

(7) (a) Deak, D. S.; Silly, F.; Porfyrakis, K.; Castell, M. R. *Nanotech* **2007**, *18*, 075301. (b) Deak, D. S.; Silly, F.; Newell, D. T.; Castell, M. R. *J. Phys. Chem. B* **2006**, *110*, 9246.

(8) Xiao, W.; Ruffieux, P.; Ait-Mansour, K.; Groning, O.; Palotas, K.; Hofer, W. A.; Groning, P.; Fasel, R. *J. Phys. Chem. B* **2006**, *110*, 21394.

(9) Barth, J. V. *Annu. Rev. Phys. Chem.* **2007**, *58*, 375.

(10) Piot, L.; Marchenko, A.; Wu, J.; Mullen, K.; Fichou, D. *J. Am. Chem. Soc.* **2006**, *127*, 16245.

(11) Bonifazi, D.; Kiebele, A.; Stöhr, M.; Cheng, F.; Jung, T.; Diederich, F.; Spillmann, H. *Adv. Funct. Mater.* **2007**, *17*, 1051.

(12) Chen, L.; Huang, H.; Zhang, H. L.; Yuhara, J.; Wee, A. T. S. *Adv. Mater.* **2008**, *20*, 484.

(13) Theobald, J. A.; Oxtoby, N. S.; Phillips, M. A.; Champness, N. R.; Beton, P. H. *Nature* **2003**, *424*, 1029.

(14) Perdigao, L. M. A.; Perkins, E. W.; Ma, J.; Staniec, P. A.; Rogers, B. L.; Champness, N. R.; Beton, P. H. *J. Phys. Chem. B* **2006**, 12539.

(15) Silly, F.; Shaw, A. Q.; Castell, M. R.; Briggs, G. A. D. *ChemComm.* **2008**, 1907.

(16) Xu, W.; Dong, M.; Gersen, H.; Rauls, E.; Vazquez-Campos, S.; Crego-Calama, M.; Reinhoudt, D. N.; Stensgaard, I.; Laegsgaard, E.; Linderoth, T. R.; Besenbacher, F. *Small* **2007**, *3*, 854.

(17) Silly, F.; Shaw, A. Q.; Porfyraris, K.; Briggs, G. A. D.; Castell, M. R. *Appl. Phys. Lett.* **2007**, *91*, 253109.

(18) Silly, F.; Shaw, A. Q.; Briggs, G. A. D.; Castell, M. R. *Appl. Phys. Lett.* **2008**, *92*, 023102.

(19) Perdigao, L. M. A.; Fontes, G. N.; Rogers, B. L.; Oxtoby, N. S.; Goretzki, G.; Champness, N. R.; Beton, P. H. *Phys. Rev. B* **2007**, *76*, 245402.

(20) Swarbrick, J. C.; Rogers, B. L.; Champness, N. R.; Beton, P. H. *J. Phys Chem. B* **2006**, *110*, 6110.

(21) Silly, F.; Weber, U. K.; Shaw, A. Q.; Burlakov, V. M.; Castell, M. R.; Briggs, G. A. D.; Pettifor, D. G. *Phys. Rev. B* ,

(22) Staniec, P. A.; Perdigao, L. M. A.; Rogers, B. L.; Champness, N. R.; Beton, P. H. *J. Phys. Chem. C* **2007**, *111*, 886.

(23) Silly, F.;FABVIEWER; http://dr-silly.atspace.com/.

(24) Barth, J. V.; Brune, H.; Ertl, G.; Behm, R. J. *Phys. Rev. B* **1990**, *42*, 9307.

(25) Zhang, H.-M.; Xie, Z.-X.; Long, L.-S.; Zhong, H.-P.; Zhao, W.; Mao, B.-W.; Xu, X.; Zheng, L.-S. *J. Phys. Chem. C* **2008**, *112*, 4209.

(26) Bohringer, M.; Schneider, W.-D.; Glockler, K.; Umbach, E.; Berndt, R. *Surf. Sci.* **1998**, *419*, L95.

(27) Ordejon, P.; Artacho, E. *Phys. Rev. B* **1996**, *53*, R10441.

(28) Soler, J. M.; Artacho, E.; Gale, J. D.; García, A.; Junquera, J.; Ordejón, P.; Sánchez-Portal, D.; J. *Phys: Condens. Matter* **1980**, *21*, 2630.

(29) Kleinman, L.; Bylander, D. M. *Phys. Rev. Lett.* **1982**, *48*, 1425.

(30) Bachelet, G. B.; Hamann, D. R.; Schlüter, M. *Phys. Rev. B* **1982**, *25*, 2103.

(31) Troullier, N.; Martins, J. L. *Phys.Rev. B* **1991**, *43*, 1993.

(32) Kleinman, L. *Phys. Rev. B* **1980**, *21*, 2630.

(33) Boys, S. F.; Bernardi, F. *Mol. Phys.* **1970**, *19*, 553.

(34) Perdew, J. P.; Burke, K.; Ernzerhof, M. *Phys. Rev. Lett.* **1996**, *77*, 3865.

(35) (a) Kelly, R. E. A.; Kantorovich, L. N. *J. Mater. Chem* **2006**, *16*, 1894. (b) Kelly, R. E. A.; Kantorovich, L. N. *J. Phys. Chem. B* **2005**, *589*, 139.

(36) Grimme, S. *J. Comput. Chem.* **2004**, *25*, 1463.

(37) Langreth, D. C.; Dion, M.; Rydberg, H.; Schröder, E.; Hyldgaard, P.; Lundqvist, B. I. *Int. J. Quantum Chem.* **2005**, *101*, 599.

(38) Piana, S.; Bilic, A. *J. Phys. Chem. B* **2006**, *110*, 23467.

JP8033769